ILLUMINATION CONDITIONS AT THE POLES OF THE MOON AND MERCURY, AND APPLICATION TO DATA ANALYSIS. Erwan Mazarico[1], Joseph B. Nicholas[2], Gregory A. Neumann[3], David E. Smith[1] and Maria T. Zuber[1]. [1] Department of Earth, Atmospheric and Planetary Sciences, Massachusetts Institute of Technology, Cambridge, MA 02139, USA (mazarico@mit.edu); [2] Emergent Space Technologies, Greenbelt MD; [3] Planetary Geodynamics Laboratory, NASA Goddard Space Flight Center, Greenbelt, MD 20771, USA.

Introduction: The Moon and Mercury both have very low obliquities (1.54 and 0.01 degrees respectively), which can locally create extreme thermal environments in their polar regions given their lack of an atmosphere. The Lunar Orbiter Laser Altimeter (LOLA) [1] and the Mercury Laser Altimeter (MLA) [2] have recently acquired precise topographic data, which enable the computational modeling of the solar illumination at their poles [3,4]. In addition to the determination of the permanently shadowed regions (PSRs) and their relationship to remote sensing data such as neutron flux observations [5] and surface albedo [4], the modeling of the illumination conditions can be helpful for mission planning and exploration in tasks such as Earth visibility and path optimization [3,6]. Here, we describe how modifications to our modeling tools can expand their usage.

Method: As outlined in [3], our approach is to precompute the angular elevation of the horizon from each point in the region of interest. This expensive but one-time computation has been parallelized to achieve larger study areas and higher resolution. The resulting horizon data allow rapid direct comparison to the elevation of a source at any time. While we typically use the Sun as a (n extended) source, we can readily perform calculations of the surface visible from the Earth. To account for a large number of sources, we have modified the program to load in memory the complete horizon dataset (which can amount to hundreds of gigabytes), because the prior assumption of the whole map being illuminated from a single direction is no longer valid. To reproduce the geometry of specific spacecraft observations, the illumination modeling only needs to be applied at each timestep over a field of view much smaller than the whole study area. Therefore, for data calibration and analysis, the increased number of temporal steps can be compensated by the limited spatial extent to be modeled.

The Moon: Algorithm improvement has allowed us to update our past results [3] over both poles (65-90°) with improved resolution (240m/pixel). The most recent LOLA maps have excellent coverage in those study areas: 85.2 and 91.2% pixels contain LOLA measurements in these north and south polar regions respectively. We find that the total area in permanent shadow was under-estimated by ~30% in previous calculations at lower resolution (480m/pixel) [7], and that ~40% of the PSRs lie outside of the 80-90° regions studied in [3].

An ancillary output of the horizon computation, the solid angle of sky visible form the surface, was used by [8] to calibrate the amount of incident UV starlight. Together with the reflected flux as measured by LAMP, the albedo of the surface at UV wavelengths can be estimated [8]. However, the UV sources are not uniformly distributed, consisting of an extended sky background, individual UV-bright stars and at times Earthshine. Modeling those various sources precisely is now achievable. Figure 1 shows an example of the total incident flux from the 1,000 brightest UV stars [9], dominated by sunlight when present (shown in white). A day's worth of LRO groundtracks is also shown. We find that the monthly (due to the Moon rotation) and seasonal (due to the LRO orbit beta angle) variability is significant.

The study of insolation-driven variability of the LEND-measured neutron counts [10] can also benefit from the modeling of actual illumination conditions over the instrument footprint, as the local solar time is not necessarily an accurate proxy for insolation in the polar regions.

Mercury: Preliminary MLA topographic maps were used by [4] to determine the relationship between

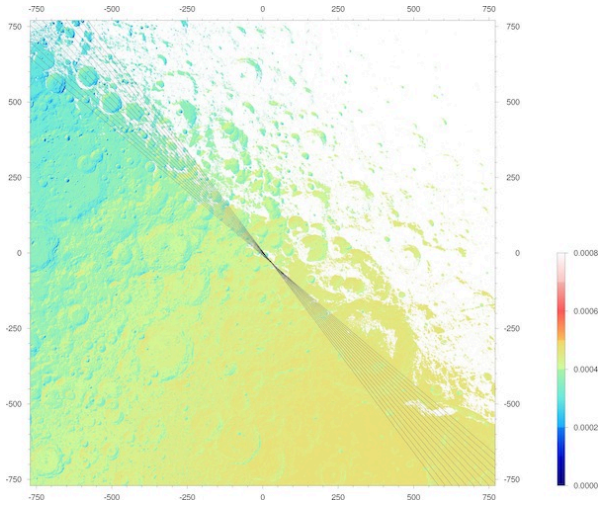

Figure 1. Map of the combined incident flux from the 1,000 brightest UV stars over the lunar south pole (65-90°S). Sunlit areas are in white. The LRO groundtrack within 12 hours of the simulated time are also shown. Stereographic projection centered on the South Pole, in km. Map units are arbitrary.

PSRs and MLA-dark deposits near Mercury's north pole, and by [11] for the modeling of its thermal environment. We used more recent maps, which contain numerous off-nadir MLA tracks over the polar region (>84°N) not sampled with the primary mission data. We compute the average illumination at 500m/pixel resolution (Figure 2), and find a few locations that appear to be in permanent sunlight. However, because the cross-track distances between MLA tracks can still be large in the immediate vicinity of the north pole, it is possible that some critical crater rim heights are under-estimated and would create artificial high-illumination point. Although one location is also illuminated with an independent, image-based topographic model (R.Gaskell), further comparison with MDIS images needs to be conducted.

To better understand the relationship between observed radar-bright deposits [12], MLA reflectance [4] and illumination conditions, we simulated the viewing geometry of the radar sessions of [12] with the MLA topography. Figure 3 shows the resulting map, a proxy to the total incident radar energy. We find that the great majority of the north pole region was well illuminated, with only the floor of a few small craters shadowed in all viewing opportunities.

References: [1] Smith D. E. et al. (2010) *GRL*, 37, L18204. [2] Zuber M. T. et al. (2013) *Science*, 336, 217-220. [3] Mazarico E. et al. (2011), *Icarus*, 211, 1066. [4] Neumann G. A. et al. (2013) *Science*, 339, 296-300. [5] Mitrofanov I. G. et al. (2010) *Science*, 330, 483-486. [6] Johnson A. W. et al. (2010), SPACE 2010 Conference, #8829. [7] Mazarico E. et al. (2011), *LEAG*, #2030. [8] Gladstone G. R. et al. (2011), *JGR*, 117, E00H04. [9] P. Miles and K. Retherford, private communication. [10] Livengood T. A. et al., AGU 2013, P51B-1733. [11] Paige et al. (2013), *Science*, 339, 300-303. [12] Harmon J. K. et al. (2011), *Icarus*, 211, 37-50. [13] Chabot N. L. et al. (2013), *JGR*, 118, 26-36.

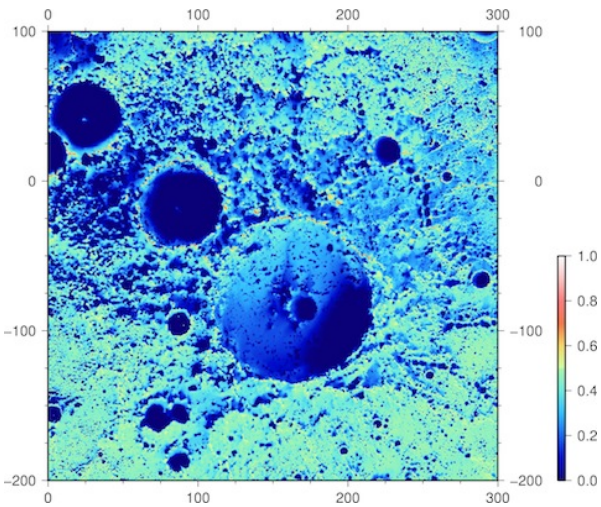

Figure 2. Map of the average solar visibility over the north pole region of Mercury (69-90°N). Stereographic projection centered on the North Pole, in km.

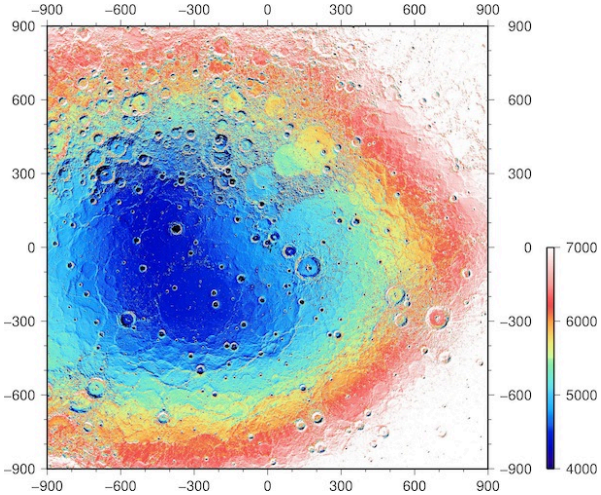

Figure 3. Map of the cumulative incident flux on the north pole region of Mercury (69-90°N) from the multiple radar looks of **[12]**. Stereographic projection centered on the North Pole, in km. Map units are arbitrary.